MICROSTRUCTURE AND PROPERTY OF REGENEPERCENTAGED SILK FIBROIN/CHITOSAN NANOFIBERS

by

Lei ZHAO [a,b*], Yuan-Fang HE [a,b], Qian-Wen WANG [a,b], and Chun-Hui HE [c,d]

[a] Yancheng Institute of Industry Technology, Yancheng, China
[b] Jiangsu Ecology Textile Engineering Technology Research & Development Center, Yancheng Institute of Industry Technology, Yancheng, China
[c] National Engineering Laboratory for Modern Silk, College of Textile and Clothing Engineering, Soochow University, Suzhou, China
[d] Nantong Bubbfil Nanotechnology Company Ltd., Nantong, China

Original scientific paper
DOI: 10.2298/TSCI1603979Z

Composite silk fibroin/chitosan nanofiber membrane was fabricated by bubbfil electrospinning. The influence of chitosan content on composite membrane's microstructure, mechanical property, and the percentage of water-dissolved were studied experimentally. The result indicated that the crystallinity of electrospun membrane was enhanced by increasing chitosan concentration. It is noteworthy that the percentage of water-dissolved was the minimum when the weight ratio of silk fibroin/chitosan was 70:30. After the composite membrane treated by the methanol, the percentage of water-dissolved of the nanofiber membrane decreased significantly. The strength and elongation at break of composite membrane increased gradually with the increased content of chitosan. Additionally, the electrospun silk fibroin/chitosan membrane showed excellent antibacterial property.

Key words: *regenepercentaged silk fibroin, chitosan, bubbfil electrospinning, microstructure, mechanical properties, antibacterial*

Introduction

Silk fibroin (SF) and chitosan (CS) are widely used as biomedical materials because of their good biocompatibility. The CS has good mechanical properties, anti-bacterial and biodegradability, and is widely used as additive to enhance mechanical property of nanofibers. This paper investigated the mechanical and anti-bacterial properties of composite SF/CS nanofiber by bubbfil electrospinning [1-7].

Experimental

In order to remove the sericin, the mulberry silk was boiled for 30 minutes at 0.1% (W/W) Na_2CO_3 solution for three times. Then pure SF was dissolved in ternary solvents of $CaCl_2$, H_2O, and C_2H_5OH (molar ratio is 1:8:2) at 75 1 °C. The solution was casted into acrylonitrile-butadine-styrene, plastic plate to achieve the dry film at room temperature after dialysis and filtration. The membrane was dissolved in formic acid with a variety of SF concentra-

* Corresponding author; e-mail: zhaolei7365@163.com

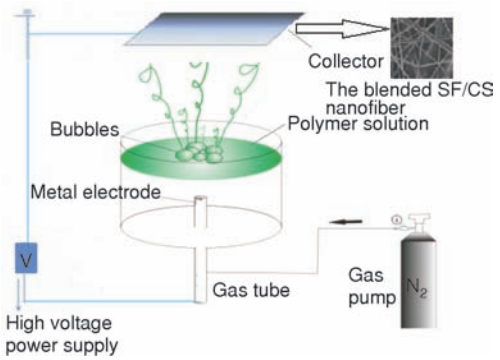

Figure 1. The bubbfil spinning

tion. The CS was dissolved in formic acid with the concentration of 3.6 wt.%. Then a certain percentage of the spinning solutions were mixed by the previous two solutions.

Figure 1 illustrates the spinning process by bubbfil electrospinning. The test of Raman spectroscopy (France Dilor's LabRam-1B micro-laser spectrometer) and DTA-TG (Diamond 5700 DTA/TG thermal analyzer) were carried out to investigate the structure and thermal properties of composite nanofiber membrane.

The as-prepared membrane and the treated membrane by methanol are dissolved in water for 1 hour at room temperature, and dried at 50 °C. Their weight before and after dissolution are measured, then the percentage of water-dissolved is determined by the equation:

$$\text{Percentage of water dissolved} = [(W_0 - W)/W_0] \times 100\% \quad (1)$$

where W_0 is the weight of the membrane before dissolving and W – the weight of the membrane after dissolving.

The thickness of fiber membrane was tested by YG (B) 141D digital fabric thickness tester using five different samples and the average thickness was calculated. Then the nanofiber membrane was tested by the YG004A electronic single fiber strength ester at the clamping length of 10 mm. Five samples are used in experiment to measure breaking strength [cN], elongation at break [mm], percentage of elongation [%] so the breaking strength [cN/mm^2] is determined by the equation:

$$\text{Breaking Strength [cN/mm}^2\text{]} = \text{Breaking Strength [cN]}/(W\,H) \quad (2)$$

where W is the width of the nanofiber membrane, and H – the thickness of the nanofiber membrane.

Results and discussions

Laser Raman spectroscopy is an effective method to study the structure of the solid and liquid protein. The experience value of amide I and amide III in the Raman spectrum is shown in tab. 1.

Table 1. The experience value of amide I and amide III in the Raman spectrum

Conformation	Amide I [cm^{-1}]	Amide III [cm^{-1}]
α-helix	1645~657	1270~1310
β-pleated sheet	1665~1680	1220~1240
Random coil	1660~1670	about 1250

Figure 2 shows the peaks of pure SF at 1666.78 cm^{-1} (amide I), 1255.12 cm^{-1} (amide III), and 1104.6 cm^{-1} (amide III), suggesting that pure SF nanofibers mainly appear random and α-helix structure with minimal β-sheet structure. While the SF/CS composite nanofibers appear

peak at 1259.76 cm^{-1} (amide III), 1667.55 cm^{-1} (amide I), and β-sheet peak at 1675.36 cm^{-1}, suggesting the increase of β-sheet structure of SF/CS nanofibers. The SF interaction with CS molecules to form hydrogen bonds contributed to the structure of fibroin transfer into β-sheet quickly.

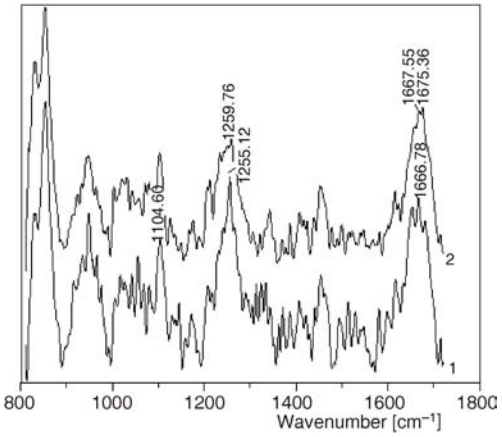

Figure 2. Laser Raman spectroscopy of SF and SF/CS composite nanofibres; 1 – Pure SF and 2 – 13% SF/CS

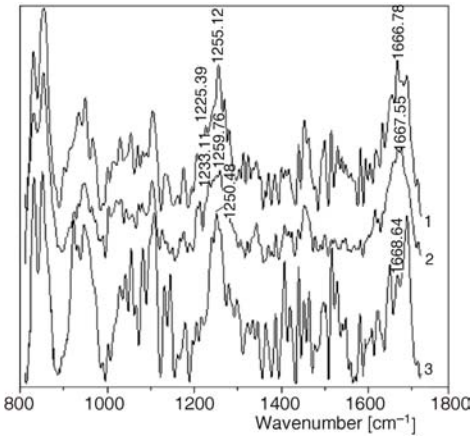

Figure 3. The Raman spectrum under different content of CS; 1 – 11% SF/CS, 2 – 13% SF/CS, and 3 – 17% SF/CS

As shown in fig. 3, the No. 1 and No. 2 shows the β-sheet peak at 1225.39 cm^{-1} and 1233.11 cm^{-1} (amide III), respectively, while the No. 3 shows the random coil structure, indicating that the degree of β-sheet of No. 1 and No. 2 is higher than that of No. 3. Additionally, the wave number of peak of amide III is less than that of No. 2. As a result, the degree of β-sheet about No. 1 is higher than that of No. 2.

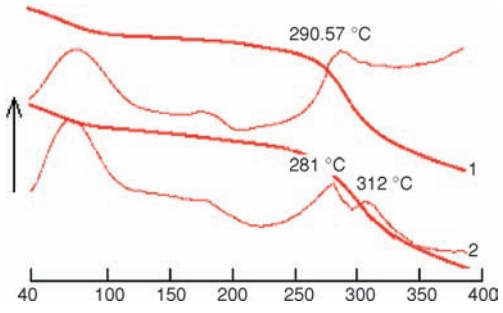

Figure 4. The DTA-TG curves of SF and SF/CS nanofibers; 1 – pure SF and 2 – 13% SF/CS

The differential thermal analysis-thermogravi metric (DTA-TG) curves of SF and SF/CS nanofibers are shown in fig. 4. From fig. 4 we can see that the SF membrane only presented endothermic peak at 290.57 °C, indicating a random structure. The SF/CS composite membrane appeared endothermic peak at 281 °C and the maximum thermal decomposition temperature rises to 312 °C, which proves that the conformation of the SF in SF/CS nanofibers transfer into β-sheet partly. The hydrogen bonds between SF and CS after the addition of CS enhanced the structure of SF transfer from the random conformation into β-sheet conformation.

As can be seen from fig. 5 that curve 1 only appear endothermic peak at 307 °C, while curve 2 and curve 3 not only appear endothermic peak at 312 °C and 310 °C but near 281 °C. Those results illustrate that SF 2 and SF 3 mainly show β-sheet with part of random conformation. Curve 1 only appears endothermic peak at 307 °C and the maximum decomposition temperature of SF 2 is slightly higher than SF 3. This indicates

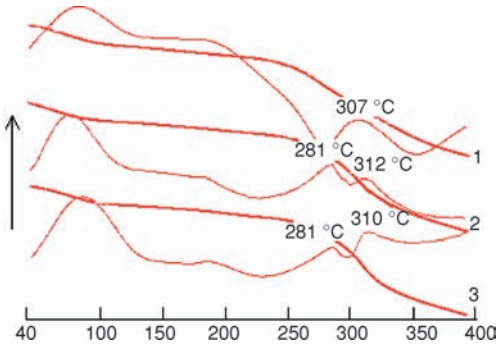

Figure 5. The DTA-TG curves under different weight ratio of SF; 1 – 11% SF/CS, 2 – 13% SF/CS, and 3 – 17% SF/CS

that the degree of β-sheet about SF 1 is higher than that of SF 2 and SF 3, and the degree of β-sheet about SF 2 is higher than that of SF 3.

The percentage of water-dissolved of the fiber membrane was shown in tab. 2. It can be seen in tab. 2 that with the increase of CS the percentage of water-dissolved of fiber membrane decreased. When the weight ratio of CF and CS is 70:30, the percentage of water-dissolved reached the minimum. The hydrogen bonds between SF and CS enhanced the degree of β-sheet and the crystallinity.

After sample 3 treated by methanol for 60 minutes, the percentage of water-dissolved decreased to 12.8%, indicating the improvement of crystallinity of treated SF. As a result, the percentage of water-dissolved of the SF/CS composite fiber membrane was reduced.

Table 2. The percentage of water-dissolved of the nanofiber membrane

No.	Samples	the percentage of water-dissolved/%
1	Pure SF	43.0
2	80/20 SF/CS composite membrane	42.0
3	70/30 SF/CS composite membrane	32.8
4	60/40 SF/CS composite membrane	34.9
5	Sample 3 treated by methanol for 60 minutes	12.8

Table 3. The mechanical of SF/CS nanofiber membrane

The mass fraction of SF [%]	17	13	11
Diameter [nm]	139	104	87
Thickness [mm]	0.246	0.282	0.236
Breaking strength [cNmm^{-2}]	132.15	168.59	181.95
Initial modulus [cNmm^{-2}]	23.42	14.88	7.61
Elongation at break [mm]	0.448	0.617	0.592
Percentage of elongation [%]	4.45	6.16	5.88

The effect of the content of the CS on the mechanical properties of SF/CS nanofiber is shown in tab. 3. It can be seen from tab. 3 that the breaking strength of the composite membrane increased due to the decrease of SF and the increase of CS. This is mainly because that the number of hydroxyl, amino groups increase with the increase of CS. As a result, the hydrogen bonding between the SF molecules and CF molecules is enhanced, resulting in the improvement of binding force within molecules. Meanwhile, the degree of β-sheet of SF improved. As a result, the strength of SF/CS nanofiber increased.

The inhibition percentage of the SF/CS composite membrane is shown in tab. 4. It can be seen from tab. 4 that the SF/CS composite membrane have excellent antibacterial activity against the *staphylococcus aureus* and *escherichia coli* while there is no antibacterial property of the SF. This is because that the quaternary ammonium cation in the CS molecules can absorb bacteria and combine with the anion on the surface of bacterial cell wall, which stop the delivery of the material inside and outside the bacterial cell wall. As a result, the proliferation and growth of the bacterial was inhibited.

Table 4. The inhibition percentage of the SF/CS composite electrospinning membrane

Samples	*Staphylococcus aureus*		*Escherichia coli*	
	6 h	24 h	6 h	24 h
SF electrospun membrane	0	0	0	0
SF/CS composite electrospun membrane	97.8	100.0	99.1	100.0

Conclusions

The hydrogen bonds between SF and CS enhanced the crystallinity of the SF/CS composite nanofiber membrane. With the increase of CS, the percentage of water-dissolved of nanofiber membrane decreased. It is noteworthy that the percentage of water-dissolved reaches the minimum when the weight ratio of SF and CS is 70:30. After the composite membrane treated by the methanol, the water-dissolved percentage of the nanofiber membrane decreased obviously. Additionally, the strength and the elongation at break of the composite membrane increase with the increase of CS. There is no antibacterial property of the SF nanofiber membrane, but the SF/CS composite electrospun membrane showed excellent antibacterial property against the *staphylococcus*, *staphylococcus aureus*, and *escherichia coli*.

Acknowledgment

The work is supported by visiting engineers program project in higher vocational colleges of Jiangsu Province (2014FG107), National Natural Science Foundation of China under Grant No. 61303236 and No.11372205, Top-Notch Academic Programs Project of Jiangsu Higher Education Institutions under Grant No. PPZY2015C254, and Science & Technology Pillar Program of Jiangsu Province under Grant No. BE2013072.

References

[1] He, C. H., *et al*., Bubbfil Spinning for Fabrication of PVA Nanofibers, *Thermal Science, 19* (2015), 2, pp. 743-746
[2] Li, Y., *et al*., Copper/PA66 Nanofibers by Bubbfil-Spinning, *Thermal Science, 19* (2015), 4, pp. 1463-1465
[3] Chen, R. X., *et al.*, Mini-Review on Bubbfil Spinning Process For Mass-Production of Nanofibers, *Materia, 19* (2014), 4, pp. 325-343
[4] Chen, R. X., *et al*., Bubbfil Spinning for Mass-Production of Nanofibers, *Thermal Science, 19* (2014), 5, pp. 1718-1719
[5] Chen, R., *et al*., Bubble Rupture in Bubble Electrospinning, *Thermal Science, 19* (2015), 4, pp. 1141-1149
[6] Liu, Z., *et al*., Tunable Surface Morphology of Electrospun PMMA Fiber Using Binary Solvent, *Applied Surface Science*, *364* (2016), Feb., pp. 516-521
[7] Liu, Z., *et al*., Active Generation of Multiple Jets for Producing Nanofibers with High Quality and High Throughput, *Materials & Design, 94* (2016), Mar., pp. 496-501

Paper submitted: December 9, 2015
Paper revised: January 7, 2016
Paper accepted: January 25, 2016